Supplementary Information

A Hierarchical Assembly Strategy for Near-Infrared Photothermal Conversion: Unconventional Heterogeneous Metalla[2]catenanes

Ye Lu,[a]* Dong Liu,[a] Yue-Jian Lin[a] and Guo-Xin Jin[a]*

[a]State Key Laboratory of Molecular Engineering of Polymers, Shanghai Key Laboratory of Molecular Catalysis and Innovative Materials, Department of Chemistry, Fudan University, 2005 Songhu road, Shanghai, 200438 (P. R. China)

E-mail: gxjin@fudan.edu.cn

Contents

Experimental Procedures

General Procedures. All reagents and solvents were purchased from commercial sources and used as supplied without additional purification unless otherwise mentioned. The starting materials $[Cp^*RhCl_2]_2$ was prepared by literature method.[S1] NMR spectra (^1H, ^{13}C, ^1H-^1H COSY and DOSY) were recorded on Bruker AVANCE I 400 or Bruker AVANCE III 400 spectrometers. Chemical shifts (δ) are expressed in ppm downfield from tetramethylsilane using the residual protonated solvent as an internal standard. Complex multiplets are noted as "m" and broad resonances as "br". Mass spectra were obtained with Micro TOF II mass spectrometer. Elemental analyses were performed on an Elementar Vario EL III analyzer. IR spectra of the solid samples (KBr tablets) in the range 400-4000 cm^{-1} were recorded on a Nicolet AVATAR-360IR spectrometer. Absorption spectra were recorded on Lambd650 UV and visible spectrophotometer.

Preparation of 3,6-di(pyridin-4-yl)thieno[3,2-b]thiophene (L_1). A flask was charged with 1.48 g (5.2 mmol) of 3,6-dibromothieno[3,2-b]thiophene, 2.5 g (18 mmol) of pyridine-4-boronic acid, 300 mg (0.33 mmol) of $Pd_2(DBA)_3$, and 225 mg (0.8 mmol) of $P(Cy)_3$ and purged with N_2. The mixture was suspended in 40 mL of deoxygenated 1,4-dioxane. A solution of 4 g (19 mmol) of K_3PO_4 in 20 mL of degassed water was added by syringe through a septum. The reaction was heated at reflux under N_2 overnight. Upon being cooled to room temperature, the mixture was poured into a separatory funnel and the lower aqueous phase removed and discarded. The dioxane layer was collected and filtered and the dioxane removed under reduced pressure. The residue was dissolved in chloroform and washed twice with 5 g of Na_2CO_3 in 25 mL of water. The chloroform solution was dried with anhydrous magnesium sulfate and the solvent removed under reduced pressure. The solid was recrystallized by ethyl acetate. 3,6-di(pyridin-4-yl)thieno[3,2-b]thiophene (**L_1**) was obtained as a brown powder in a 50.8 % yield (0.77 g). ^1H NMR (400 MHz, $CDCl_3$, ppm): δ = 8.74 (d, *J* = 6 Hz, 4H, Py-H), 7.83 (s, 2H, thiophene-H), 7.66 (d, *J* = 6 Hz, 2H, Py-H); Anal. calcd for $C_{16}H_{10}N_2S_2$: C 65.28, H 3.42, N 9.52, found: C 65.22, H 3.48, N 9.48.

Preparation of 3,6-di(pyridin-4-yl)-2,5-dihydropyrrolo[3,4-c]pyrrole-1,4-dione (L_2). A solution of t-BuOK (1.35 g, 12.0 mmol) in t-amyl alcohol (15 mL) is heated at 100 ˚C for 1 h under N_2. 4-cyanopyridine (1.04 g, 10.0 mmol) is added to the solution, which becomes purple. To this mixture, a solution of diethyl succinate (0.87 g, 5.0 mmol) in tert-amyl alcohol (15 mL) is added dropwise over a period of 30 min. The purple mixture is heated at 100 ˚C for additional 3 h before cooling to 50 ˚C, when a solution of MeOH:H_2O (10 mL:10 mL) is added to the reaction mixture. The resulting sluggish deep red solution is heated for 1 h under reflux and then cooled at room temperature,

and poured onto dilute HCl (1 N, 30 mL) and ice (50 g). The mixture is stirred vigorously for 30 min and the precipitate was collected by filtration. The solid is dissolved in hot MeOH (100 mL) and heated for 15 min, and then precipitate is collected and dried to afford the compound as red powder (1.2 g, 82.3%). ^{1}H NMR (400 MHz, d_6-DMSO, ppm)): δ = 10.73 (s, 2H, N-H), 8.88 (d, *J* = 6 Hz, 2H, Py-H), 8.36 (d, *J* = 6 Hz, 2H, Py-H); Anal. calcd for $C_{16}H_{10}N_4O_2$: C 66.20, H 3.47, N 19.32, found: C 66.25, H 3.41, N 19.38.

Preparation of Homo-1. A CH_3OH solution of $[Cp^*RhCl_2]_2$ (124 mg, 0.2 mmol) was added to a solution of 2,5-dihydroxycyclohexa-2,5-diene-1,4-dione (28 mg, 0.2 mmol) and NaOH (16 mg, 0.4 mmol) in CH_3OH (40 mL), and the suspension was stirred at room temperature for 6 h. AgOTf (102.8 mg, 0.4 mmol) was added to the mixture and stirred for 3 h, followed by filtration to remove insoluble compounds (AgCl and NaCl). 2,5-di(pyridin-4-yl)thieno[3,2-b]thiophene (**L_1**) (58.8 mg, 0.2 mmol) was then added to the filtrate. After the solution was stirred at room temperature for 12 h, the reaction mixture was concentrated to a volume of 3 mL under reduced pressure, filtered through Celite and recrystallized by slow diffusion of diethyl ether into the filtrate (including several drops of DMSO). A brown crystalline solid was obtained in 92.3% yield (222.67 mg); ^{1}H NMR (400 MHz, CD_3OD, ppm): δ = 8.48 (d, *J* = 4.8 Hz 8H, Py-H), 8.24 (d, *J* = 4.8 Hz 8H, Py-H), 7.97 (s, 4H, thiophene-H), 7.52 (d, *J* = 4.8 Hz 8H, Py-H), 7.11 (d, *J* = 4.8 Hz 8H, Py-H), 7.00 (br, 4H, thiophene-H), 6.03 (d, *J* = 8.0 Hz 4H, benzoquinone-H), 5.93 (d, *J* = 8.0 Hz 4H, benzoquinone-H), 1.85 (s, 60H, Cp*-H), 1.70 (s, 60H, Cp*-H); ^{13}C NMR (400 MHz, CD_3OD, ppm): δ = 183.78, 183.73, 183.67, 183.59, 183.47, 151.57, 151.36, 142.66, 142.56, 142.32, 142.17, 137.06, 137.45, 136.24, 129.56, 129.44, 129.38, 128.48, 128.42, 127.44, 127.29, 122.87, 122,79, 122.41, 122.29, 122.07, 118.90, 101.87, 101.83, 101.79, 101.64, 101.57, 7.56 (Cp*-C), 7.25 (Cp*-C); Anal. calcd for $C_{176}H_{168}F_{24}N_8O_{40}Rh_8S_{16}$: C 43.79, H 3.51, N 2.31, found: C 43.70, H 3.57, N 2.39; ESI-MS *m*/*z*: [**Homo-1**-3OTf]$^{3+}$ Calcd. 1459.6803, found 1459.6796; IR (KBr disk, cm^{-1}) *v* = 1611, 1532, 1378, 1258, 1164, 1032, 831, 639.

Preparation of Homo-2. The synthesis of **Homo-2** was carried out similarly to that of **Homo-1** with the use of 3,6-di(pyridin-4-yl)-2,5-dihydropyrrolo[3,4-c]pyrrole-1,4-dione (**L_2**) (58.2 mg, 0.2 mmol) instead of 2,5-di(pyridin-4-yl)thieno[3,2-b]thiophene (**L_1**). A rufous crystalline solid was obtained in 90.7% yield (218.04 mg); ^{1}H NMR (400 MHz, CD_3OD, ppm): δ = 8.31 (d, *J* = 4.8 Hz, 16H, Py-H), 8.11 (br, 8H, Py-H), 7.72 (br, 8H, Py-H), 5.88 (s, 4H, benzoquinone-H), 5.77 (s, 4H, benzoquinone-H), 1.86 (s, 60H, Cp*-H), 1.68 (s, 60H, Cp*-H); ^{13}C NMR (400 MHz, CD_3OD, ppm): δ = 184.06, 183.94, 183.86, 183.64, 183.50, 183.46, 160.80, 159.66, 152.05, 151.96, 151.92, 151.82, 151.76, 151.65, 141.76, 141.42, 136.22, 136.13, 135.82, 123.50, 123.41, 123.30, 121.99, 118.81, 115.45, 115.07, 102.21, 101.68, 100.99, 7.68 (Cp*-C), 7.34 (Cp*-C); Anal. calcd for $C_{176}H_{168}F_{24}N_{16}O_{48}Rh_8S_8$: C 43.94, H 3.52, N

4.66, found: C 44.01, H 3.59, N 4.58; ESI-MS *m*/*z*: [**Homo-2**-3OTf]$^{3+}$ Calcd. 1454.4169, found 1454.4168; IR (KBr disk, cm^{-1}) v = 1599, 1496, 1377, 1258, 1164, 1031, 836, 639.

Preparation of Heteo-3. Stirring a 3:1 mixture of **Homo-1** (17.38 mg, 3.6 μmol) and **Homo-2** (5.78 mg, 1.2 μmol) in NMR tube with 0.6 ml CD_3OD at room temperature during 12 h. The reaction mixture was filtered through Celite and recrystallized by slow diffusion of diethyl ether into the filtrate (including several drops of DMF). A black crystalline solid was obtained in 88.1% yield (20.41 mg); ^{1}H NMR (400 MHz, CD_3OD, ppm): δ = 8.51(br), 8.47 (br), 8.34 (m), 8.30 (m), 8.26 (m), 7.96 (s), 7.95 (s), 7.54 (br), 7.50 (m), 7.18 (m), 7.10 (m), 6.00 (s, benzoquinone-H), 5.95 (br, benzoquinone-H), 5.93 (s benzoquinone-H), 5.92 (s, benzoquinone-H), 1.83 (s, Cp*-H), 1.68 (s, Cp*-H); Anal. calcd for $C_{176}H_{168}F_{24}N_{10}O_{42}Rh_8S_{14}$: C 43.82, H 3.51, N 2.90, found: C 43.89, H 3.44, N 2.98; ESI-MS *m*/*z*: [**Heteo-3**-2OTf]$^{2+}$ Calcd. 2262.0227, found 2262.0310; IR (KBr disk, cm^{-1}) v = 1611, 1532, 1376, 1259, 1165, 1032, 832, 640.

Preparation of Heteo-4. The synthesis of **Heteo-4** was carried out similarly to that of **Heteo-3** with the feed ratio of 3:1 instead of 1:3. A black crystalline solid was obtained in 90.2% yield by slow diffusion of diethyl ether into mixture solution of CD_3OD / d_7-DMF (1:2 v/v) (21.40 mg); ^{1}H NMR (400 MHz, CD_3OD: d_7-DMF = 5:10, ppm): δ = 8.49 (d, J = 4.8 Hz, Py-H), 8.42 (s), 8.38 (br), 8.29 (d, J = 4.8 Hz, Py-H), 8.25 (s), 8.11 (br), 8.02 (br), 7.48 (d, J = 4.8 Hz, Py-H), 5.39(br, benzoquinone-H), 1.38 (s, Cp*-H), 1.34 (s, Cp*-H), 1.32 (br, Cp*-H); Anal. calcd for $C_{182}H_{182}F_{24}N_{16}O_{48}Rh_8S_{10}$ (including two DMF molecule): C 44.07, H 3.70, N 4.52, found: C 43.98, H 3.77, N 4.62; ESI-MS *m*/*z*: [**Heteo-4**-3OTf]$^{3+}$ Calcd. 1455.7324, found 1455.7375; IR (KBr disk, cm^{-1}) v = 1612, 1532, 1377, 1258, 1162, 1031, 838, 641.

Crystallographic Details. Crystallographic data for complexes **Hetero-3**, **Hetero-4**, **Homo-1** and **Homo-2** were collected using a CCD-Bruker SMART APEX system ($Ga_{K\alpha}$, λ = 1.34138 Å). Indexing was performed using APEX 2 (difference vectors method). Data integration and reduction were performed using SaintPlus 6.01. Absorption correction was performed by the multiscan method implemented in SADABS. The structures were solved and refined using SHELXTL-97. The single-crystal X-ray diffraction data of **Hetero-3**, **Hetero-4**, **Homo-1** and **Homo-2** have been deposited in the Cambridge Crystallographic Data Centre under accession number CCDC: 1946051 (**Homo-1**), 1946991 (**Homo-2**), 1946053 (**Hetero-3**), 1946054 (**Hetero-4**) (Table S1-S4).

Photothermal Conversion Properties Measurement. Crystal and solution sample were put in a PP tube. The 730 nm laser beam (Changchun New Industries optoelectronics Tech Co., Ltd. China) irradiated at a power density of 0.5 W/cm^2. And the temperature was measured with an IR thermal camera (FLIR A310 infrared camera).

Calculation of the photothermal conversion efficiency. Following the reported method,[S2] the photothermal conversion efficiency (η_T) was calculated using equation:

$$\eta_T = \frac{hA\Delta T_{max}}{I(1 - 10^{A_{730}})}$$

Here, h is the heat transfer coefficient, A is the surface area of the container, and the value of hA can be obtained from cooling curve (Figure S36). T_{max} is the maximum temperature change, which can be obtained from Figure 4a. I is the laser power (0.5 W/cm^2) and A_{730} is the absorbance of the samples at the wavelength of 730 nm.

Scheme

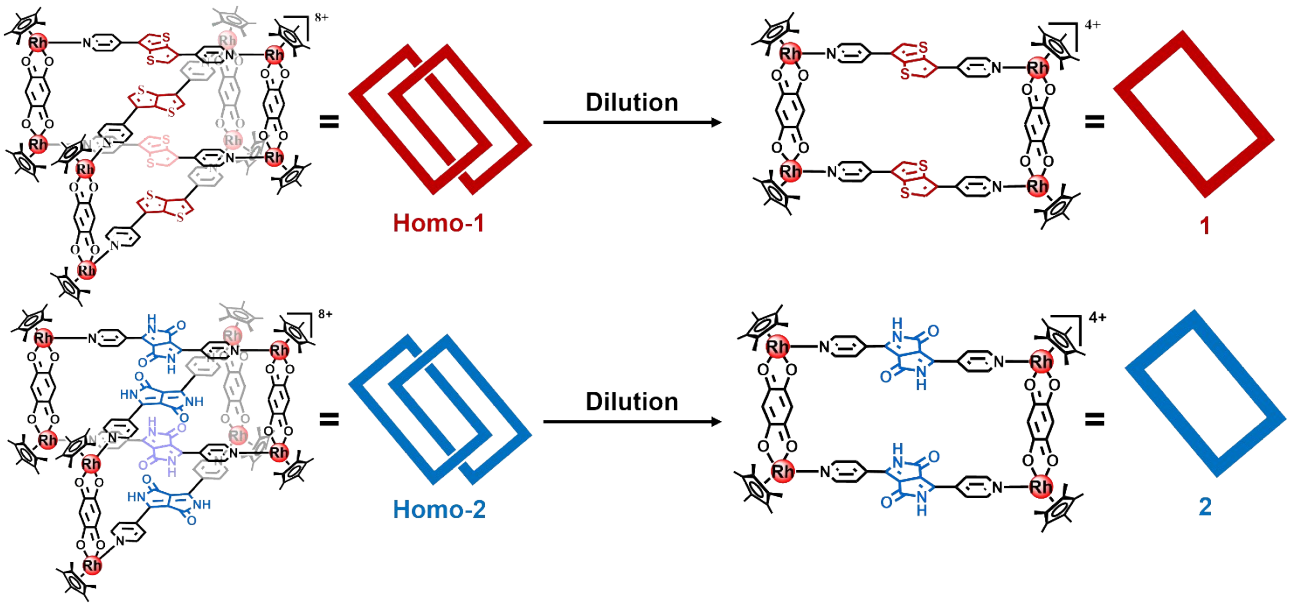

Scheme S1. The transformation from homo-[2]-catenanes to corresponding monomeric rectangle (MR).

NMR spectrum

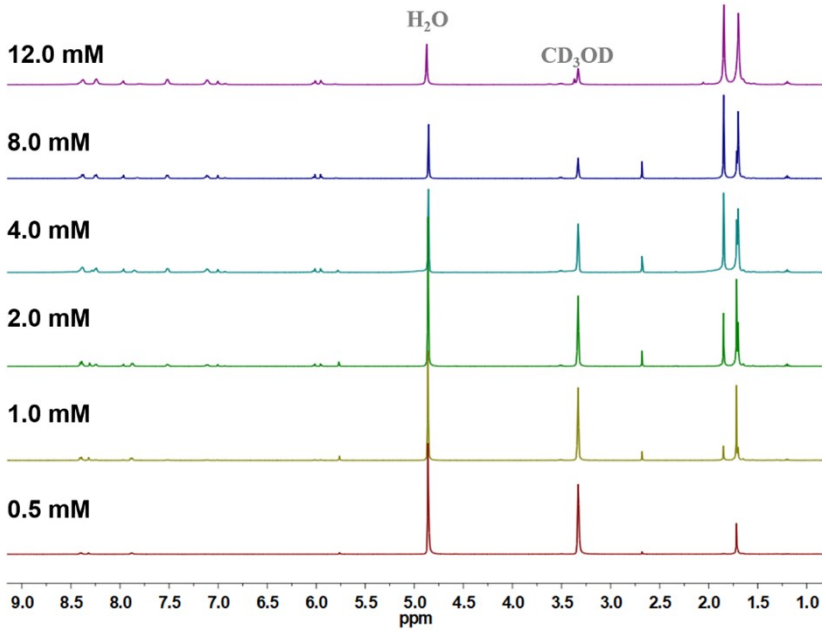

Figure S1. ^{1}H NMR spectrum of **1** and **1** + **Homo-1** in CD_3OD ([12.0 mM], [8.0 mM], [4.0 mM], [2.0 mM], [1.0 mM], [0.5 mM] 298K, 400 MHz).

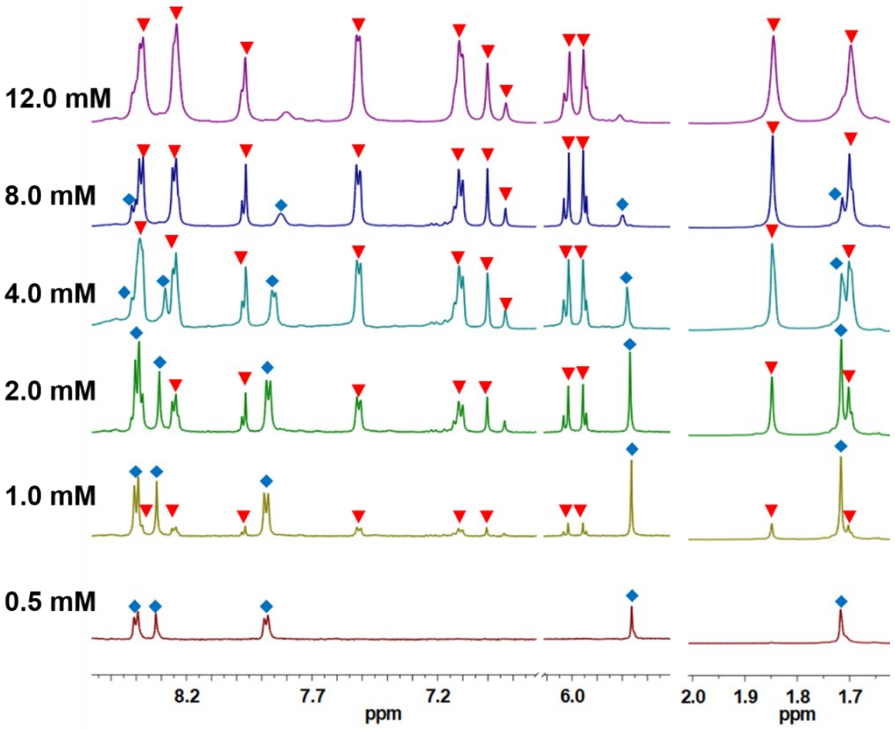

Figure S2. Partial ^{1}H NMR spectrum of **1** (◆) and **1** (◆) + **Homo-1** (▼) in CD_3OD ([12.0 mM], [8.0 mM], [4.0 mM], [2.0 mM], [1.0 mM], [0.5 mM] 298K, 400 MHz). By increasing the concentration (from 0.5 to 12.0 mM), the proportion of **Homo-1** in methanol solution also increased.

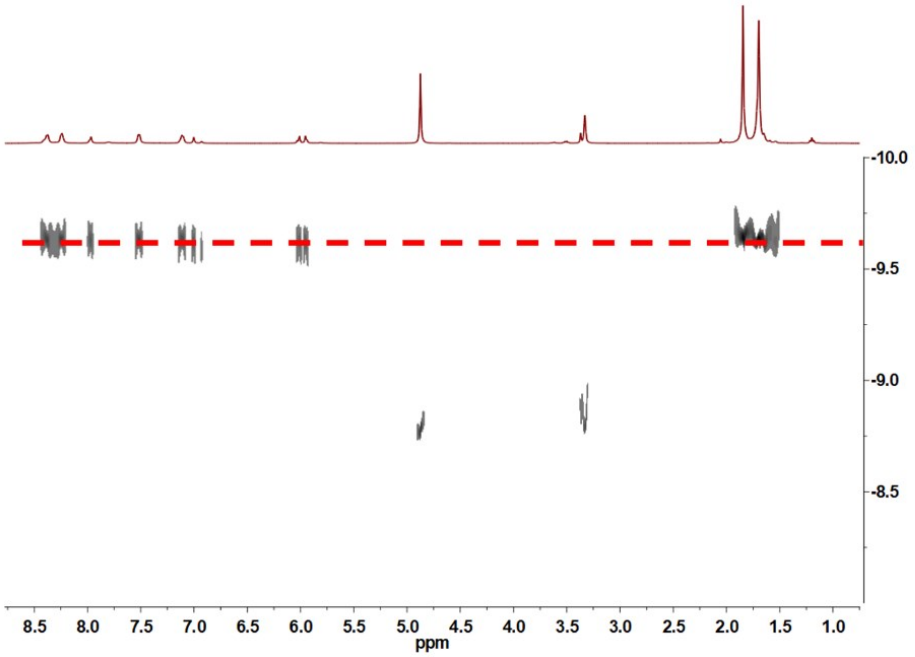

Figure S3. ^{1}H DOSY NMR spectrum of **Homo-1** (CD_3OD, [12.0 mM], 298 K, 400 MHz)

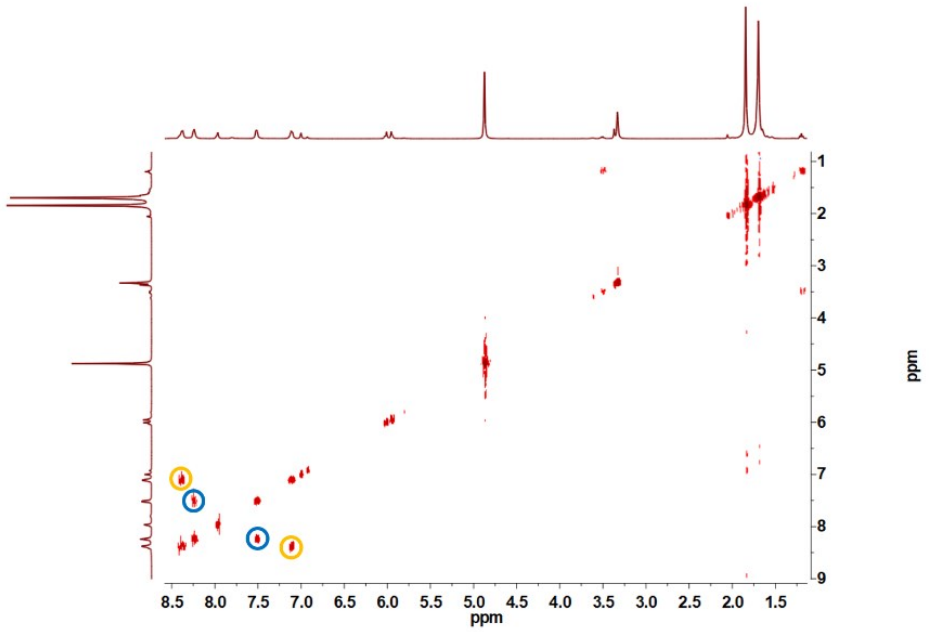

Figure S4. ^{1}H -^{1}H COSY NMR spectrum of **Homo-1** (CD_3OD, [12.0 mM], 298 K, 400 MHz)

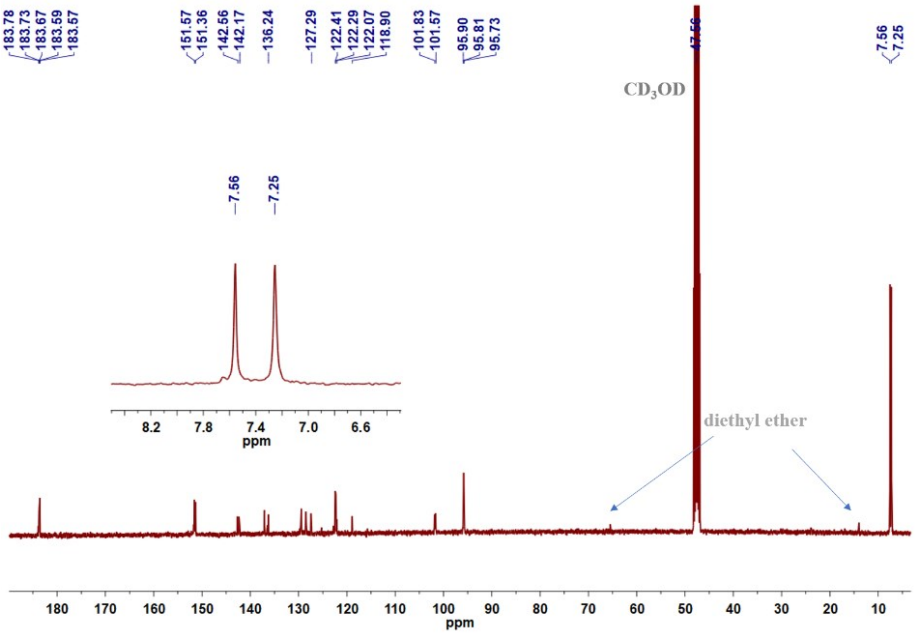

Figure S5. ^{13}C NMR spectrum of **Homo-1** (CD_3OD, [12.0 mM], 298 K, 400 MHz), there are two different Cp* group in methanol solution, which is in agreement with the result of ^{1}H NMR.

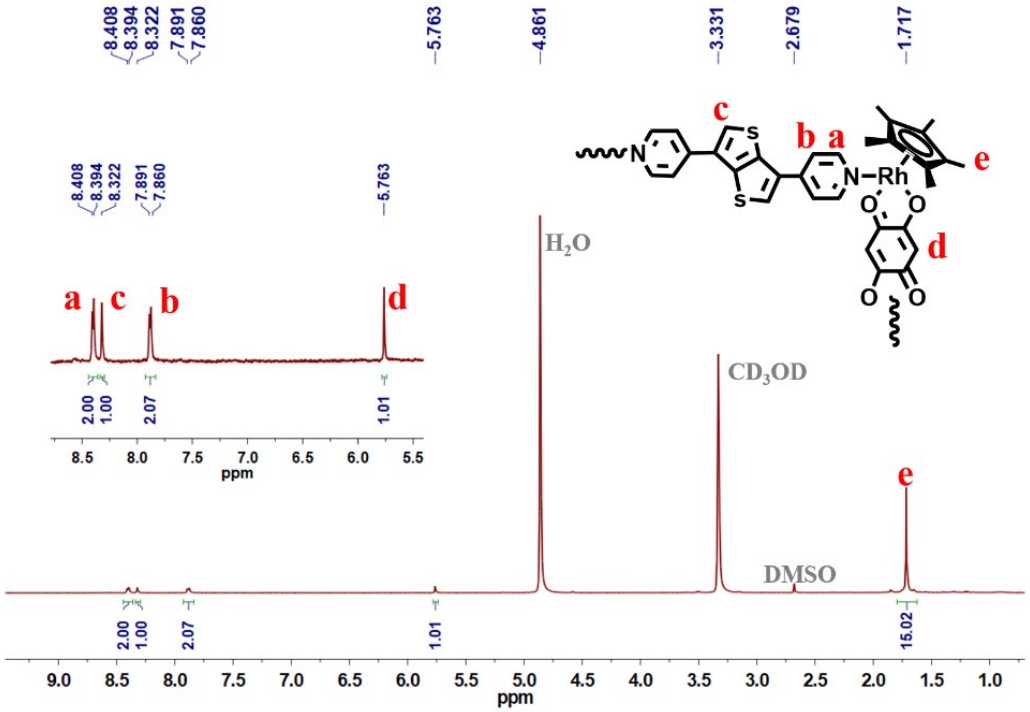

Figure S6. ^{1}H NMR spectrum of **1** (CD_3OD, [0.5 mM], 298 K, 400 MHz)

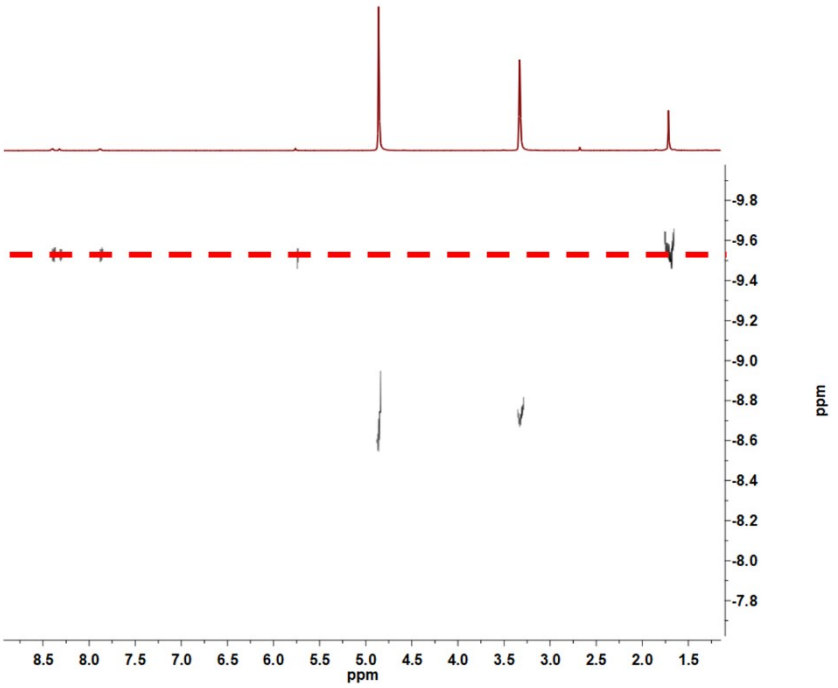

Figure S7. ^{1}H DOSY NMR spectrum of **1** (CD_3OD, [0.5 mM], 298 K, 400 MHz)

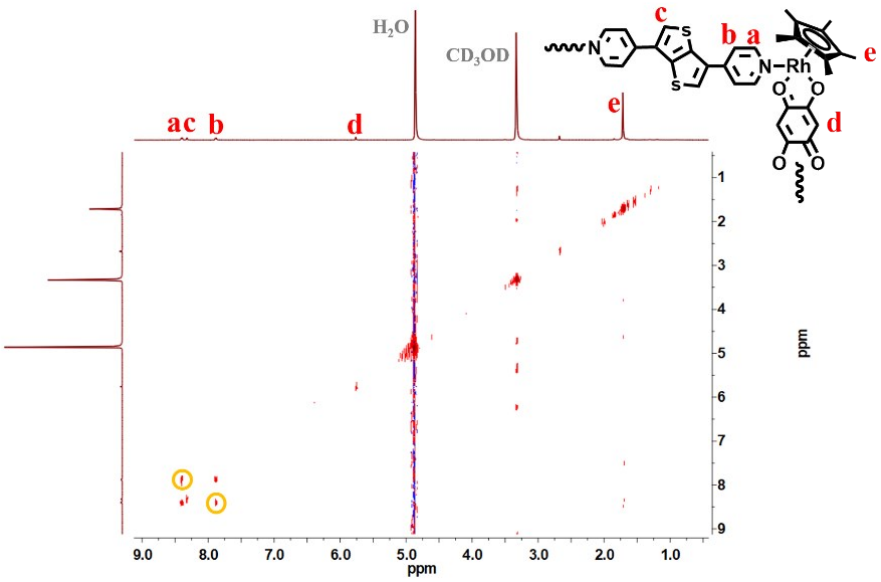

Figure S8. ^{1}H -^{1}H COSY NMR spectrum of **1** (CD_3OD, [0.5 mM], 298 K, 400 MHz)

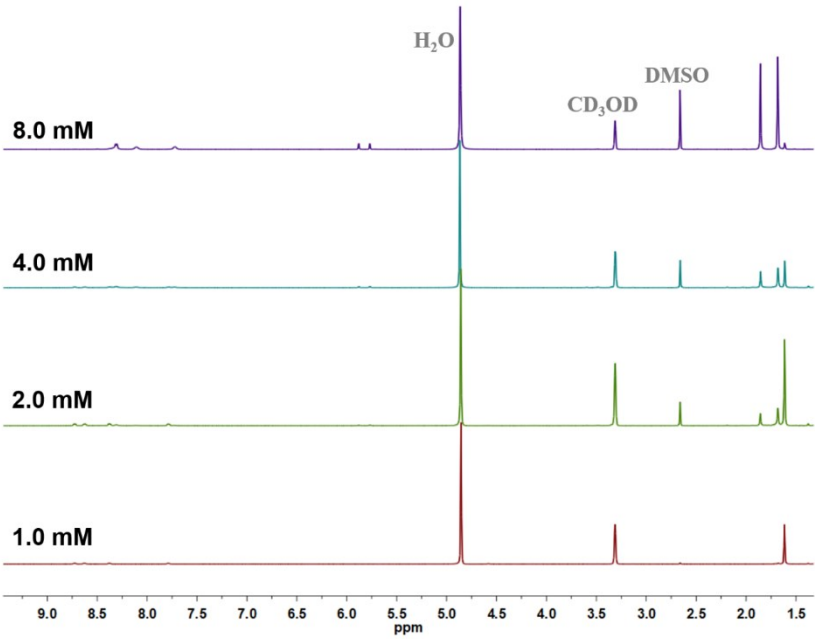

Figure S9. ^{1}H NMR spectrum of **2** and **2** + **Homo-2** in CD_3OD ([8.0 mM], [4.0 mM], [2.0 mM], [1.0 mM], 298K, 400 MHz).

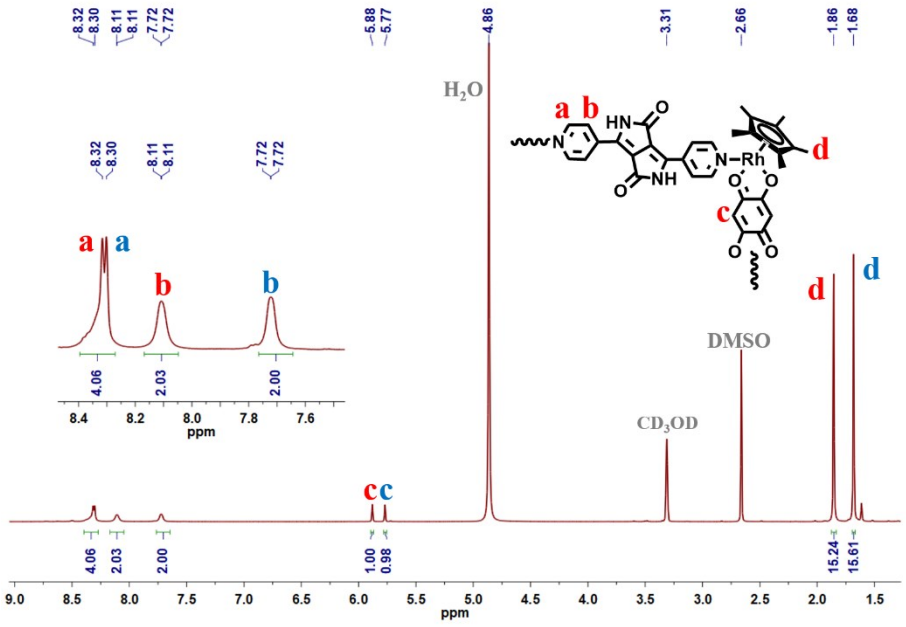

Figure S10. ^{1}H NMR spectrum of **Homo-2** in CD_3OD ([8.0 mM], 298K, 400 MHz).

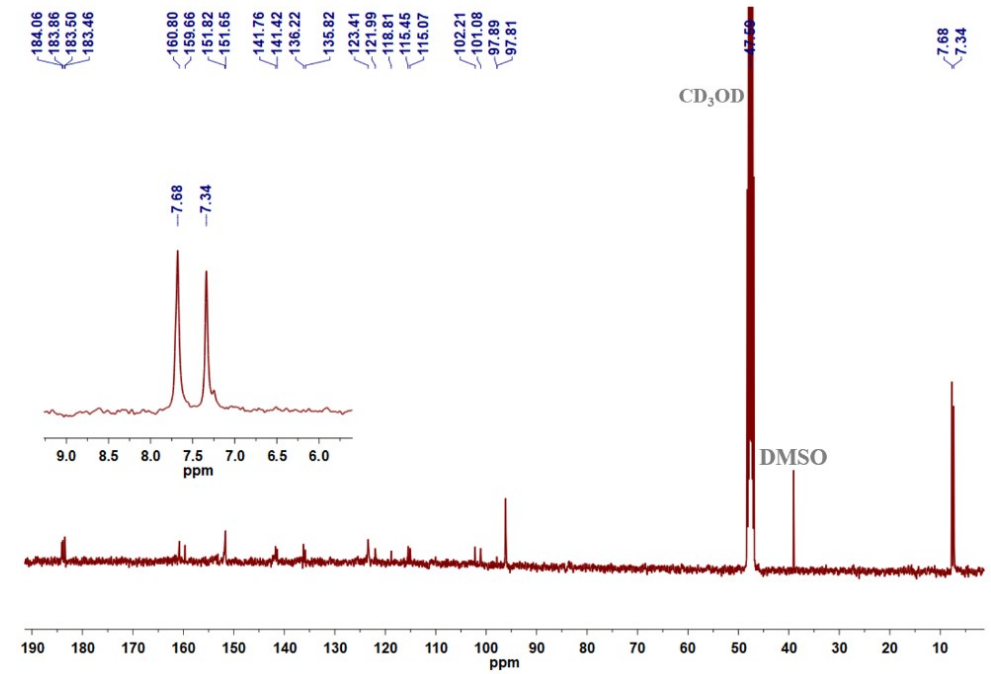

Figure S11. ^{13}C NMR spectrum of **Homo-2** (CD_3OD, [8.0 mM], 298 K, 400 MHz), there are two different Cp* group in methanol solution, which is in agreement with the results of ^{1}H NMR.

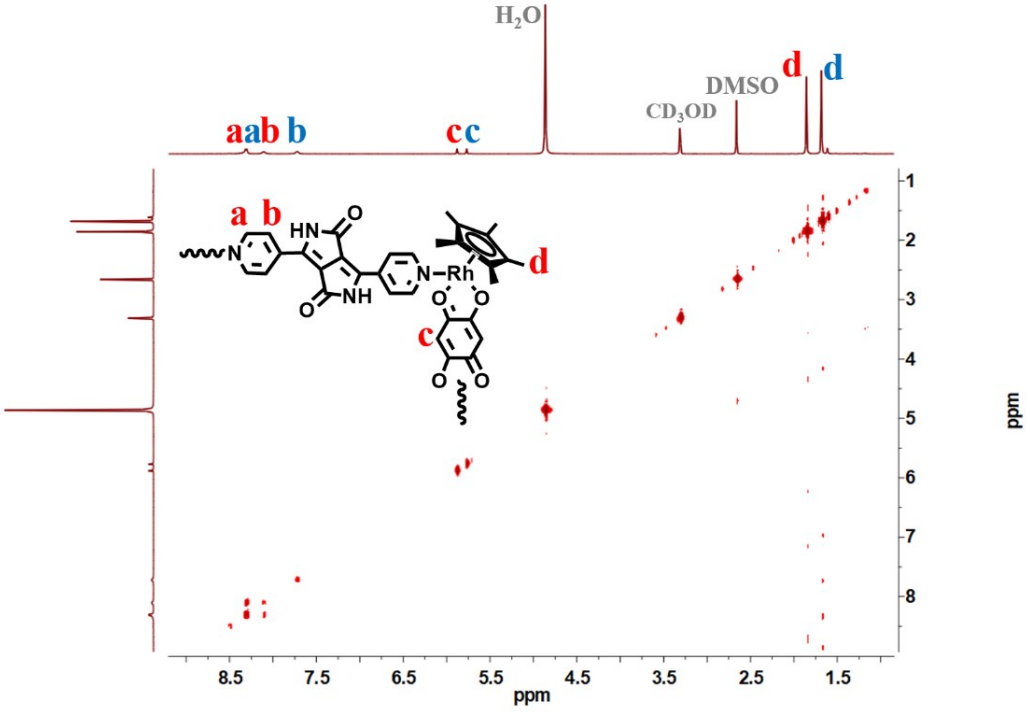

Figure S12. ^{1}H -^{1}H COSY NMR spectrum of **Homo-2** (CD_3OD, [8.0 mM], 298 K, 400 MHz)

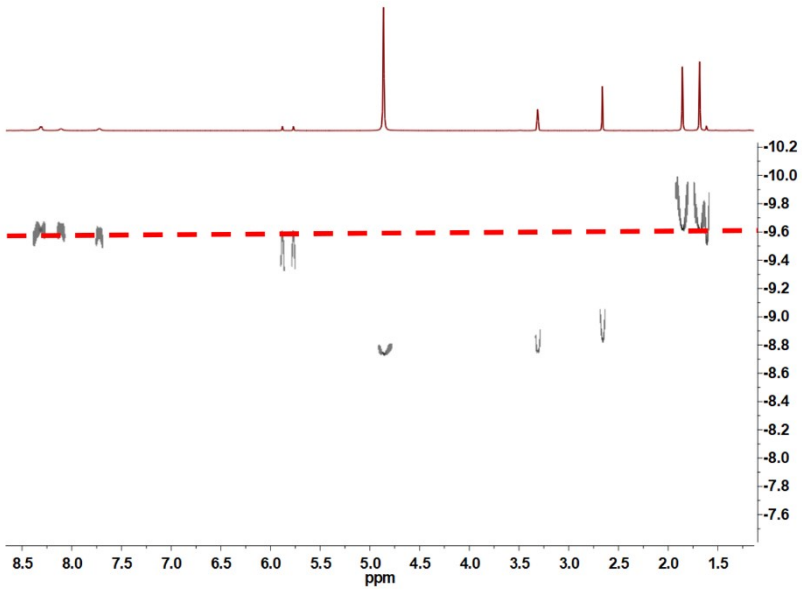

Figure S13. ^{1}H DOSY NMR spectrum of **Homo-2** (CD_3OD, [8.0 mM], 298 K, 400 MHz)

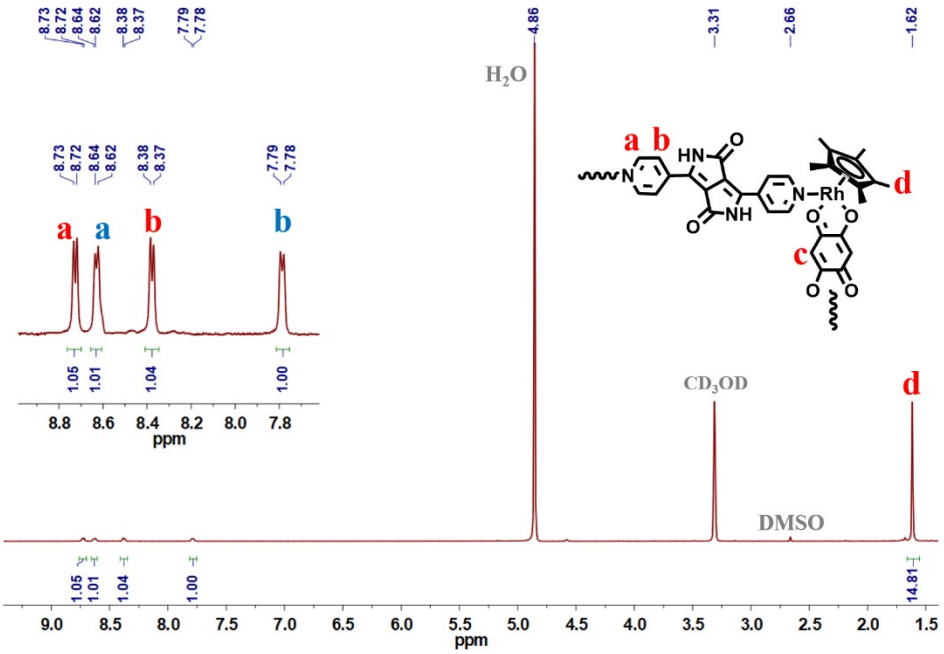

Figure S14. ^{1}H NMR spectrum of **2** in CD_3OD ([1.0 mM], 298K, 400 MHz). There are two group of the signal of pyridyl group, but there is only one group of the signal of Cp* group. The reason maybe is that two pyridyl group display trans-configuration in monomeric rectangle, similar situation has been reported in our previous work.[S3] And then, the DOSY NMR further prove that size of the MR **2** is smaller than interlocked **Homo-2** (Figure S16).

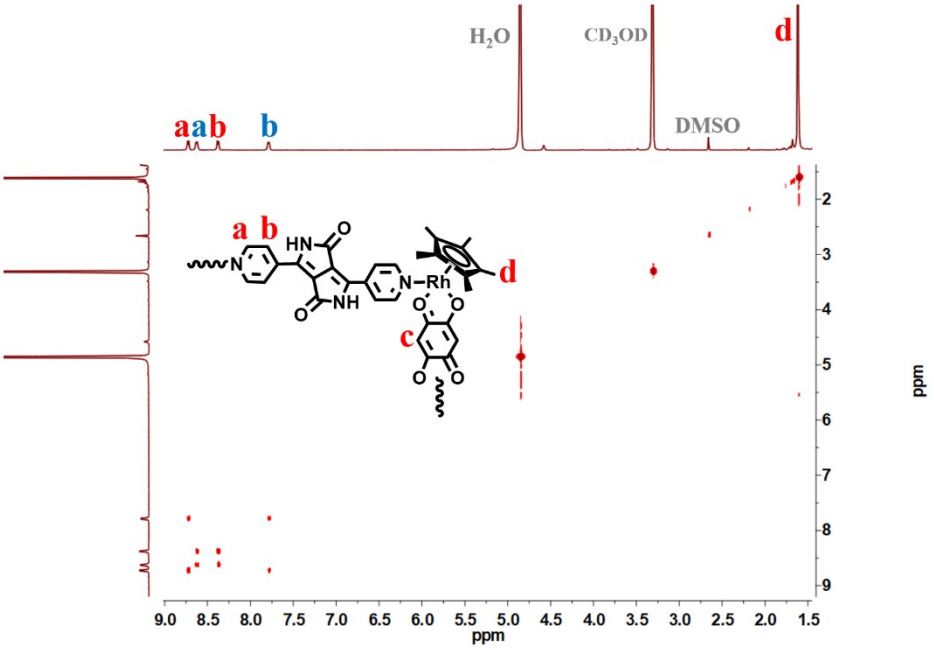

Figure S15. ^{1}H -^{1}H COSY NMR spectrum of **2** (CD_3OD, [1.0 mM], 298 K, 400 MHz)

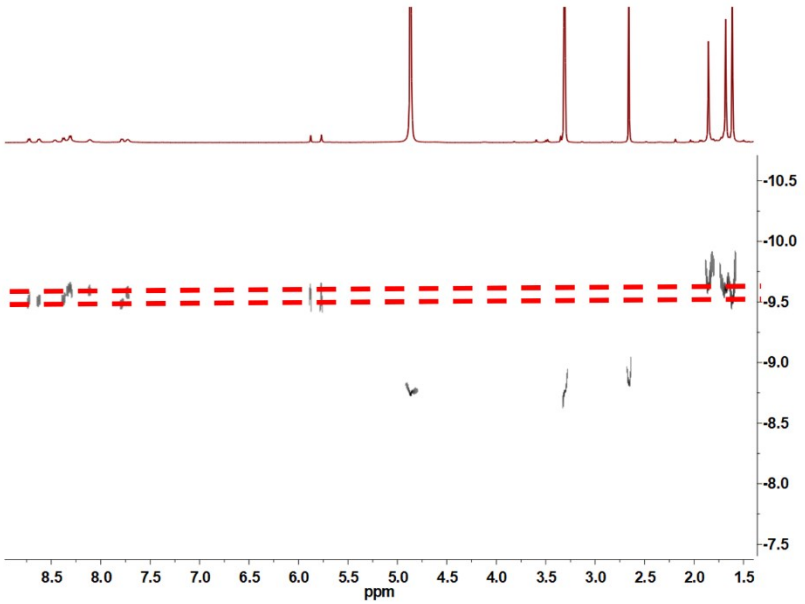

Figure S16. ^{1}H DOSY NMR spectrum of **2** + **Homo-2** (CD_3OD, [4.0 mM], 298 K, 400 MHz), the higher red line is **Homo-2** and the lower red line is **2**.

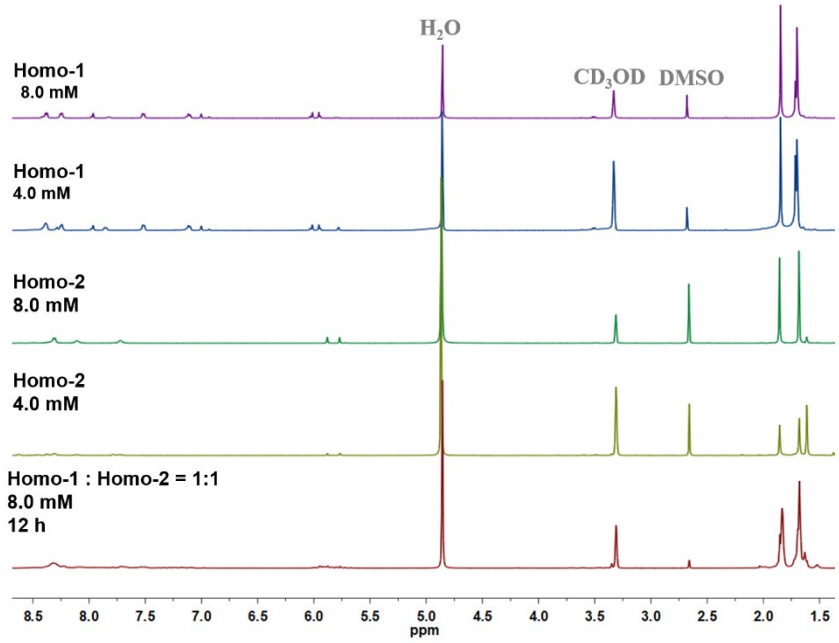

Figure S17. ^{1}H NMR spectrum of **Homo-1** + **1** (CD_3OD, 8.0 mM), **Homo-1** + **1** (CD_3OD, 4.0 mM), **Homo-2** + **2** (CD_3OD, 8.0 mM), **Homo-2** + **2** (CD_3OD, 4.0 mM) and **Homo-1** + **Homo-2** (the ratio of **Homo-1**: **Homo-2** is 1:1, 12 h) (CD_3OD, 8.0 mM)

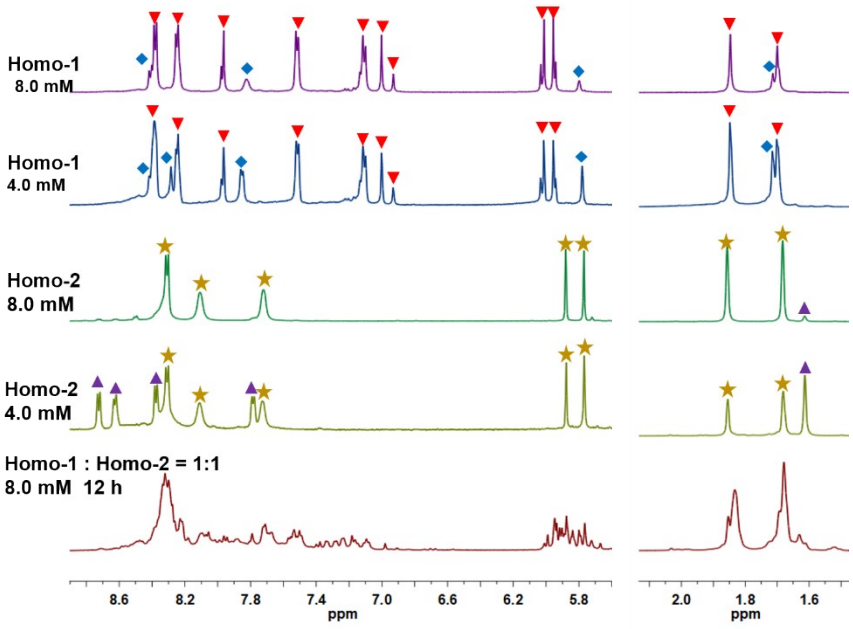

Figure S18. Partial ^{1}H NMR spectrum of **Homo-1** (▼) + **1** (◆) (CD_3OD, 8.0 mM), **Homo-1** (▼) + **1** (◆) (CD_3OD, 4.0 mM), **Homo-2** (★) + **2** (▲) (CD_3OD, 8.0 mM), **Homo-2** (★) + **2** (▲) (CD_3OD, 4.0 mM) and **Homo-1** + **Homo-2** (the ratio of **Homo-1**: **Homo-2** is 1:1, 12 h) (CD_3OD, 8.0 mM)

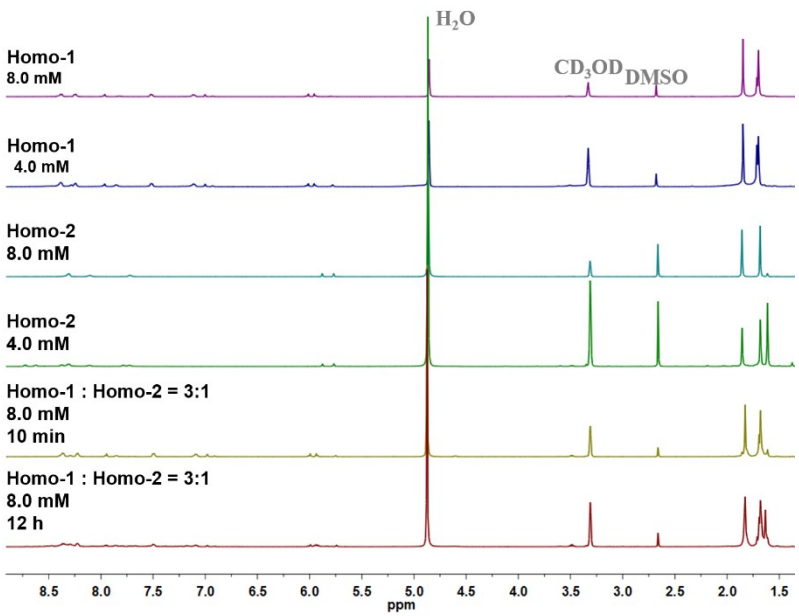

Figure S19. ^{1}H NMR spectrum of of **Homo-1** + **1** (CD_3OD, 8.0 mM), **Homo-1** + **1** (CD_3OD, 4.0 mM), **Homo-2** + **2** (CD_3OD, 8.0 mM), **Homo-2** + **2** (CD_3OD, 4.0 mM), **Homo-1** + **Homo-2** (the ratio of **Homo-1**: **Homo-2** is 3:1, 10 min) (CD_3OD, 8.0 mM) and **Homo-1** + **Homo-2** (the ratio of **Homo-1**: **Homo-2** is 3:1, 12 h) (CD_3OD, 8.0 mM)

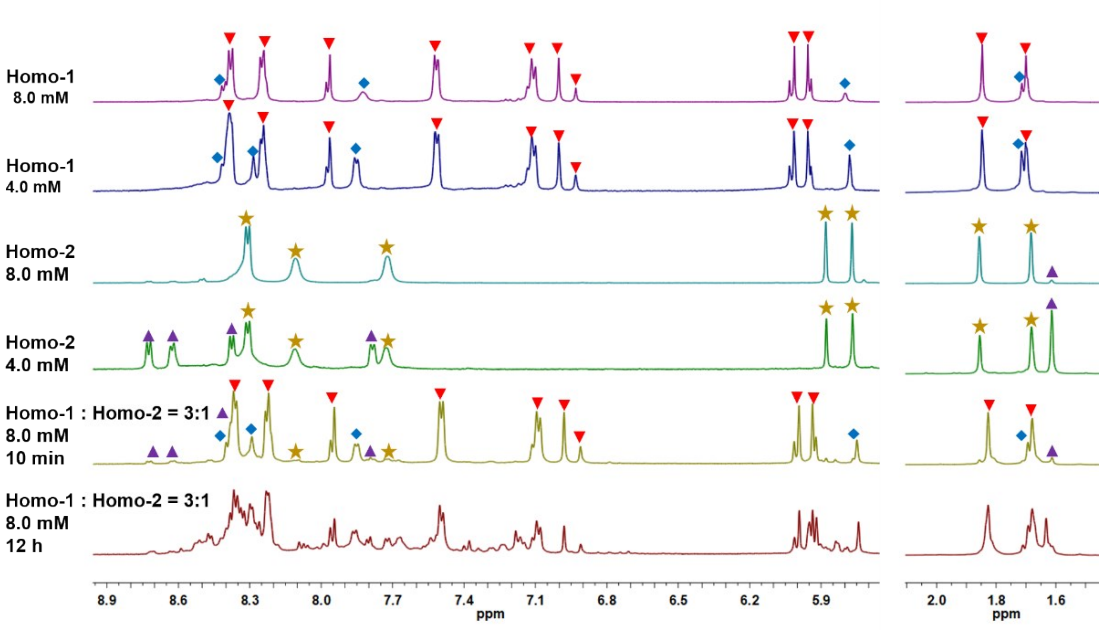

Figure S20. Partial ^{1}H NMR spectrum of **Homo-1** (▼) + **1** (◆) (CD_3OD, 8.0 mM), **Homo-1** (▼) + **1** (◆) (CD_3OD, 4.0 mM), **Homo-2** (★) + **2** (▲) (CD_3OD, 8.0 mM), **Homo-2** (★) + **2** (▲) (CD_3OD, 4.0 mM), **Homo-1** + **Homo-2** (the ratio of **Homo-1**: **Homo-2** is 3:1, 10 min) (CD_3OD, 8.0 mM) and **Homo-1** + **Homo-2** (the ratio of **Homo-1**: **Homo-2** is 3:1, 12 h) (CD_3OD, 8.0 mM)

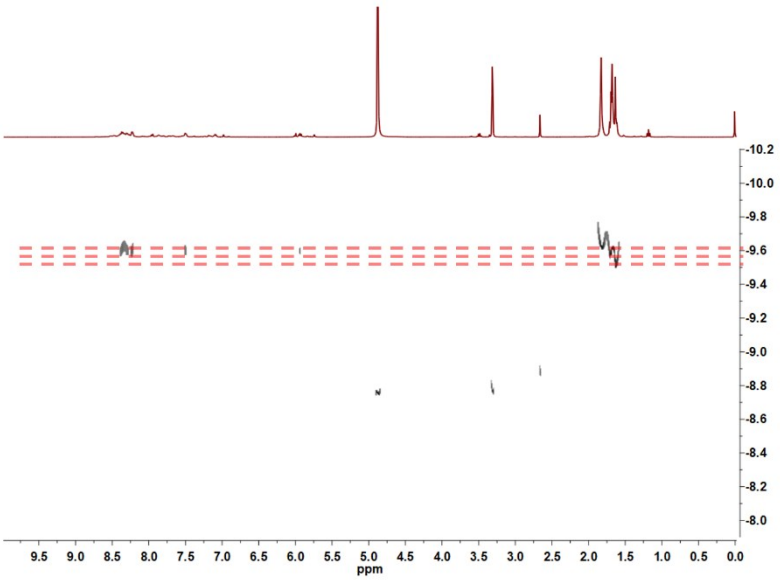

Figure S21. ^{1}H DOSY NMR spectrum of **Homo-1** + **Homo-2** at 12 h (the ratio of **Homo-1**: **Homo-2** is 3:1, 12 h) (CD_3OD, 8.0 mM, 298 K, 400 MHz). There are three kind of complex in the solution. The diffusion coefficient of main product is larger than others. That means the molecular size of main product is biggest among the three complexes.

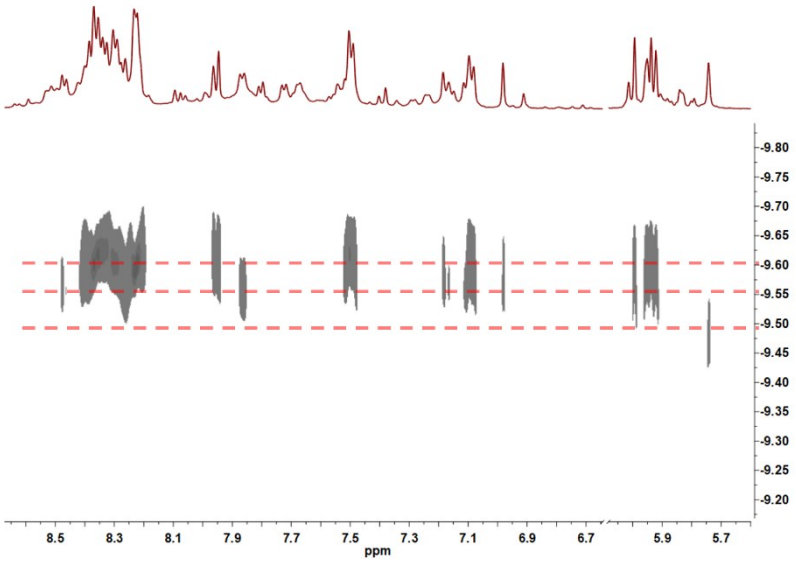

Figure S22. Partial ^{1}H DOSY NMR spectrum of **Homo-1** + **Homo-2** at 12 h (the ratio of **Homo-1**: **Homo-2** is 3:1, 12 h) (CD_3OD, 8.0 mM, 298 K, 400 MHz)

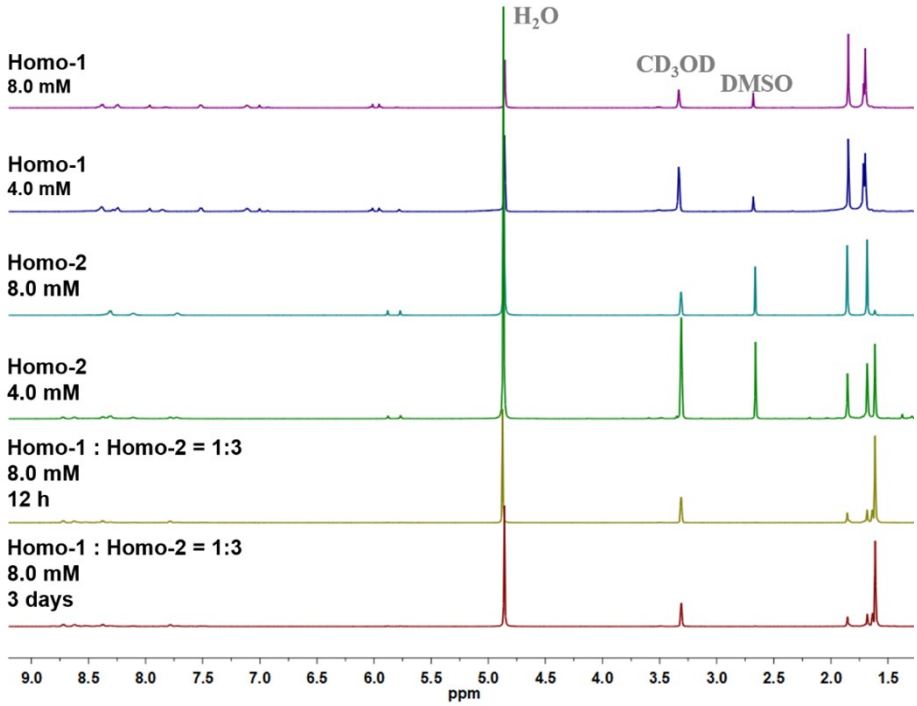

Figure S23. ^{1}H NMR spectrum of of **Homo-1** + **1** (CD_3OD, 8.0 mM), **Homo-1** + **1** (CD_3OD, 4.0 mM), **Homo-2** + **2** (CD_3OD, 8.0 mM), **Homo-2** + **2** (CD_3OD, 4.0 mM), **Homo-1** + **Homo-2** (the ratio of **Homo-1**: **Homo-2** is 1:3, 12 h) (CD_3OD, 8.0 mM) and **Homo-1** + **Homo-2** (the ratio of **Homo-1**: **Homo-2** is 1:3, 3 days) (CD_3OD, 8.0 mM)

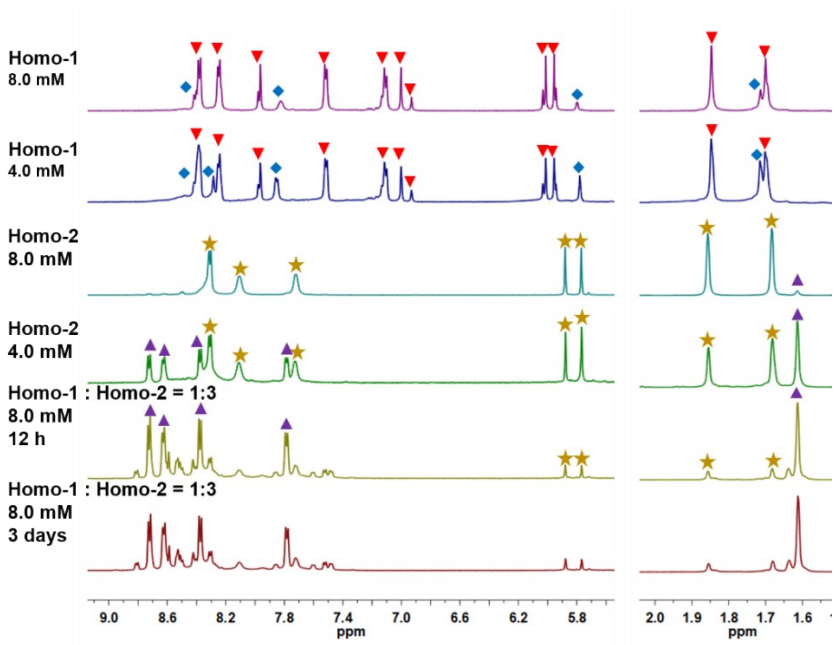

Figure S24. Partial ^{1}H NMR spectrum of **Homo-1** (▼) + **1** (◆) (CD_3OD, 8.0 mM), **Homo-1** (▼) + **1** (◆) (CD_3OD, 4.0 mM), **Homo-2** (★) + **2** (▲) (CD_3OD, 8.0 mM), **Homo-2** (★) + **2** (▲) (CD_3OD, 4.0 mM), **Homo-1** + **Homo-2** (the ratio of **Homo-1**: **Homo-2** is 1:3, 12 h) (CD_3OD, 8.0 mM) and **Homo-1** + **Homo-2** (the ratio of **Homo-1**: **Homo-2** is 1:3, 3 days) (CD_3OD, 8.0 mM).

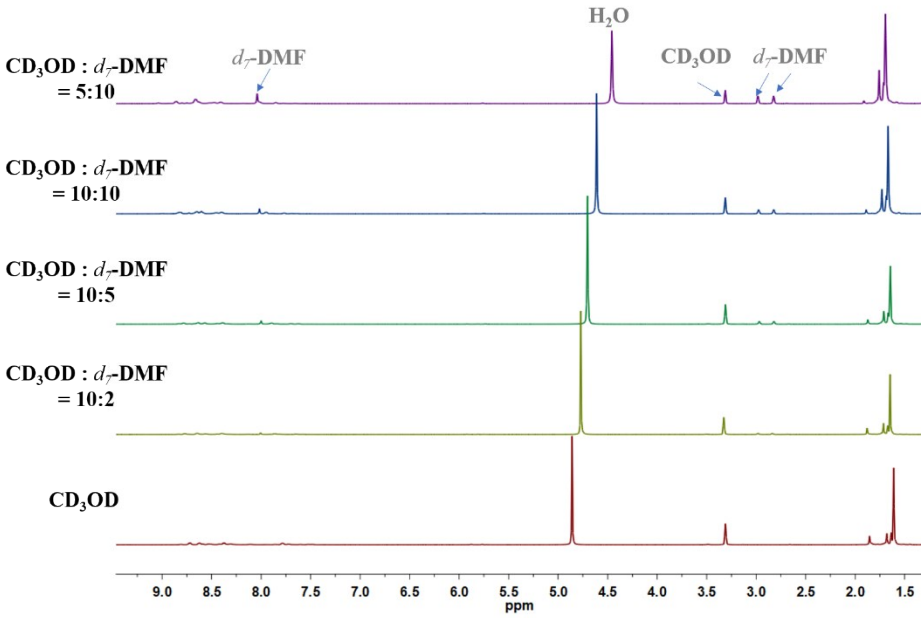

Figure S25. ^{1}H NMR spectrum of **Homo-1** + **Homo-2** (the ratio of **Homo-1**: **Homo-2** is 1:3) in CD_3OD, CD_3OD and d_7-DMF (CD_3OD: d_7-DMF = 10:2), CD_3OD and d_7-DMF (CD_3OD: d_7-DMF = 10:5), CD_3OD and d_7-DMF (CD_3OD: d_7-DMF = 10:10), CD_3OD and d_7-DMF (CD_3OD: d_7-DMF = 5:10) (8.0 mM)

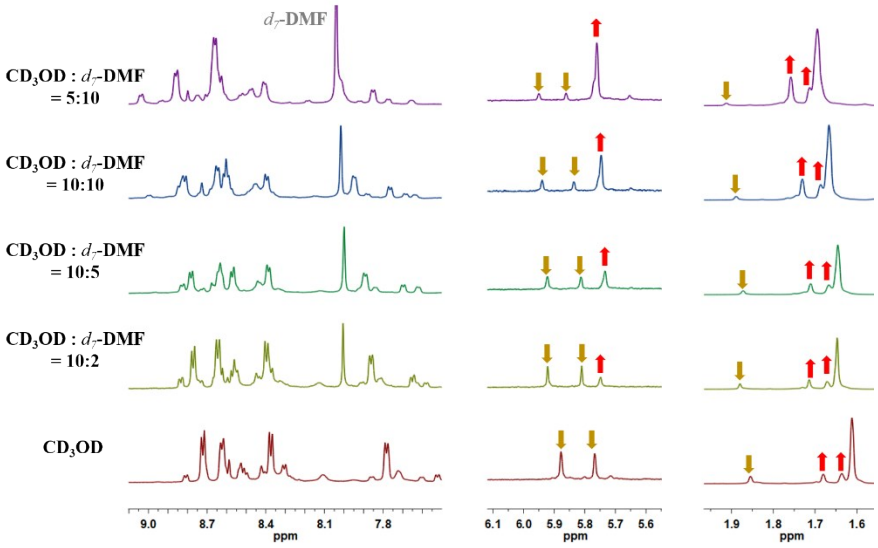

Figure S26. Partial ^{1}H NMR spectrum of **Homo-1** + **Homo-2** (the ratio of **Homo-1**: **Homo-2** is 1:3) in CD_3OD, CD_3OD and d_7-DMF (CD_3OD: d_7-DMF = 10:2), CD_3OD and d_7-DMF (CD_3OD: d_7-DMF = 10:5), CD_3OD and d_7-DMF (CD_3OD: d_7-DMF = 10:10), CD_3OD and d_7-DMF (CD_3OD: d_7-DMF = 5:10) (8.0 mM)

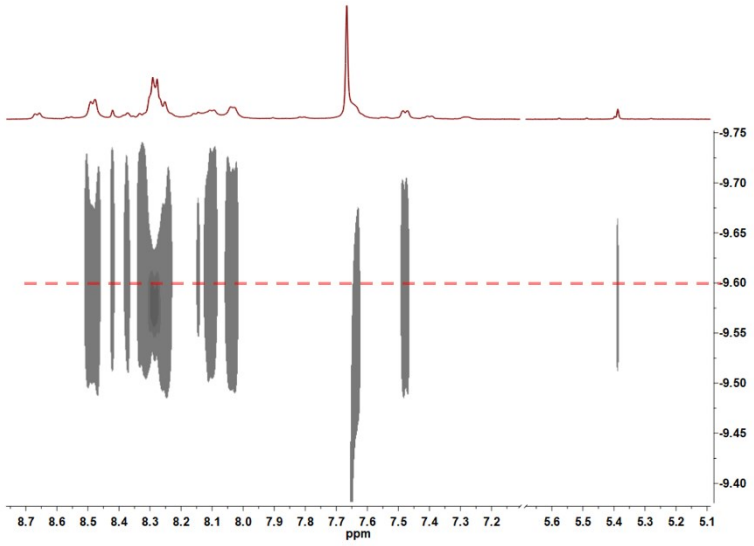

Figure S27. Partial ^{1}H DOSY NMR spectrum of **Homo-1** + **Homo-2** (the ratio of **Homo-1**: **Homo-2** is 1:3) (CD_3OD: d_7-DMF = 5:10, 8.0 mM, 298 K, 400 MHz)

ESI-MS:

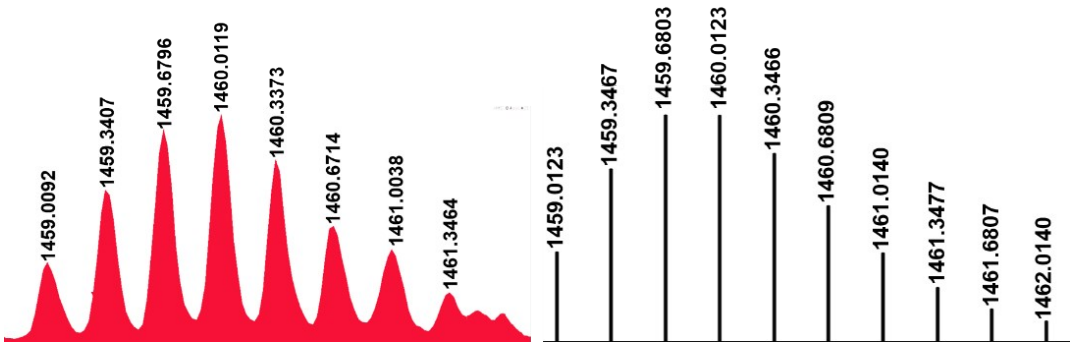

Figure S28. Experimental (right) and calculated (left) ESI-MS spectra of [**Homo-1** - 3OTf]$^{3+}$.

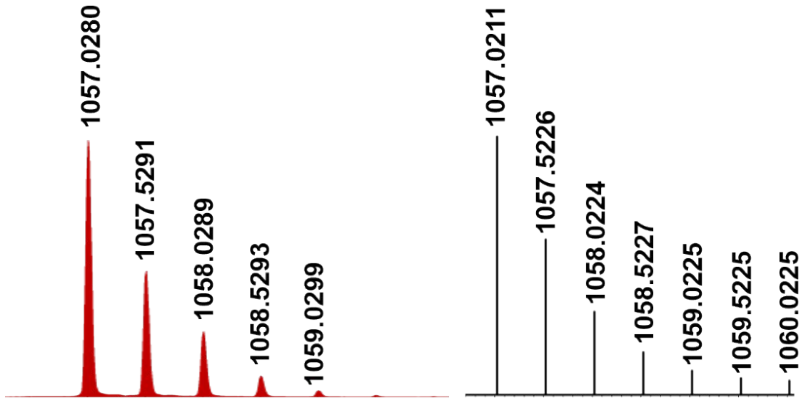

Figure S29. Experimental (right) and calculated (left) ESI-MS spectra of [**1** - 2OTf]$^{2+}$.

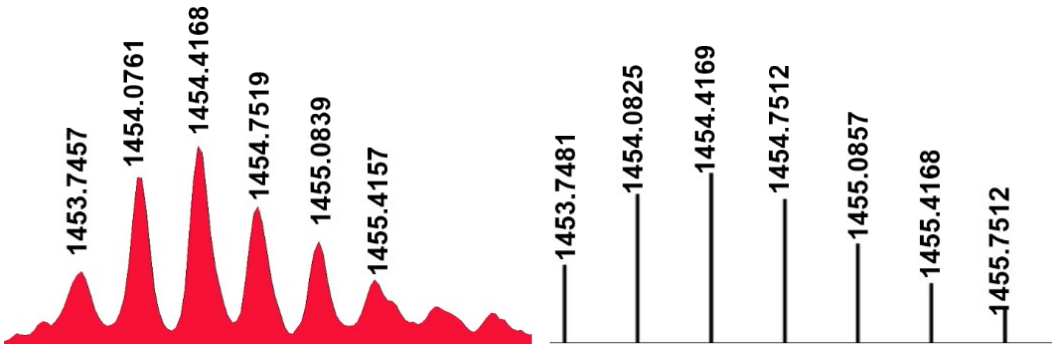

Figure S30. Experimental (right) and calculated (left) ESI-MS spectra of [**Homo-2** - 3OTf]$^{3+}$.

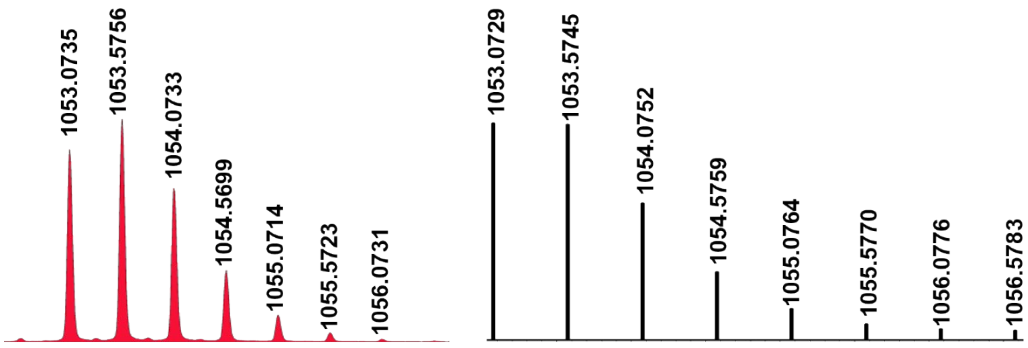

Figure S31. Experimental (right) and calculated (left) ESI-MS spectra of [**2** - 2OTf]$^{2+}$.

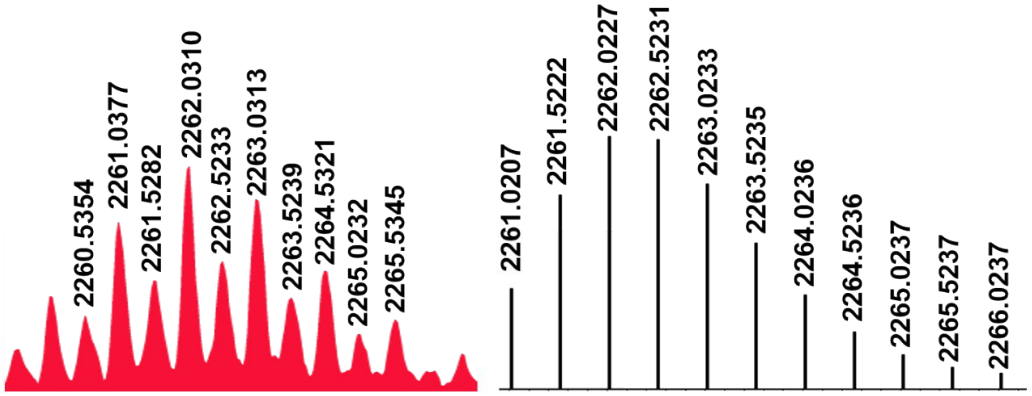

Figure S32. Experimental (right) and calculated (left) ESI-MS spectra of [**Hetero-3** - 2OTf]$^{2+}$.

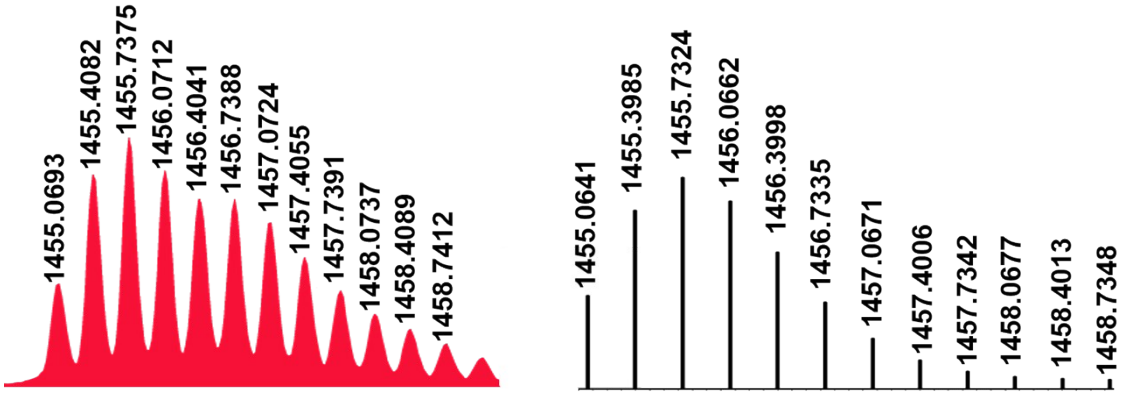

Figure S33. Experimental (right) and calculated (left) ESI-MS spectra of [**Hetero-4** - 3OTf]$^{3+}$.

Absorption spectra:

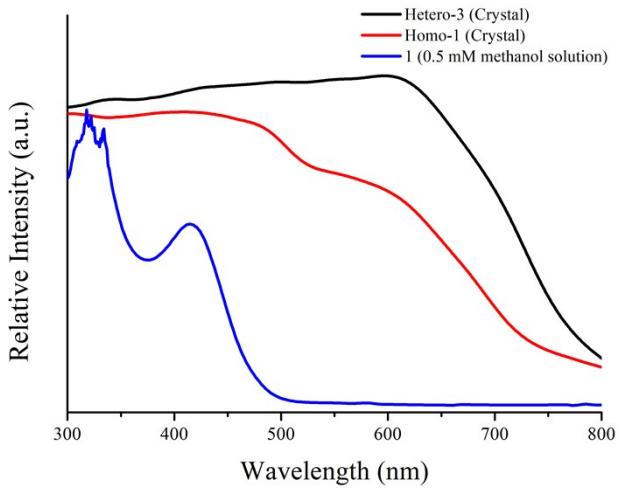

Figure S34. Absorption spectra of **Hetero-3** (Crystal), **Homo-1** (Crystal) and MR **1** (0.5 mM methanol solution)

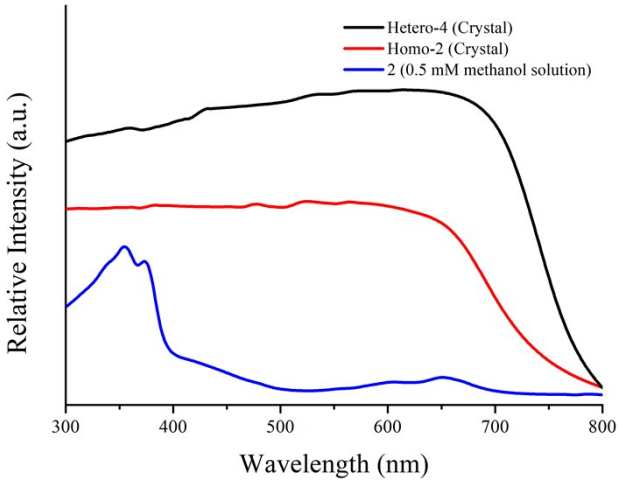

Figure S35. Absorption spectra of **Hetero-4** (Crystal), **Homo-2** (Crystal) and MR **2** (0.5 mM methanol solution)

Cooling curve

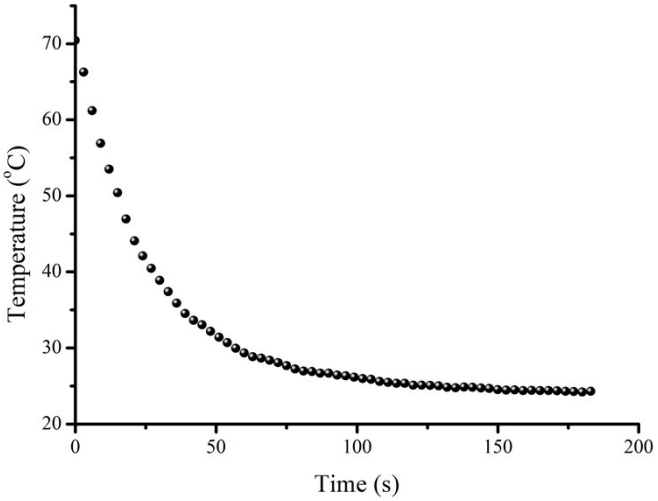

Figure S36. Cooling curve of **Hetero-4** (crystal)

Single-crystal X-ray structures

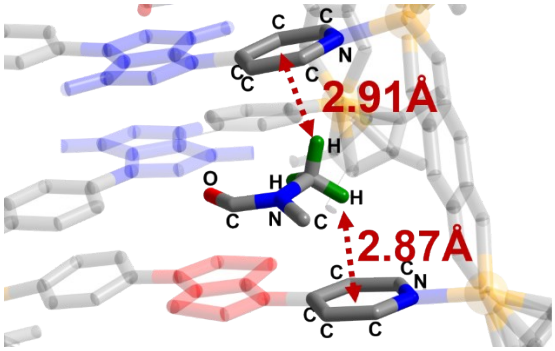

Figure S37. Partial single-crystal X-ray structures of **Hetero-4**, the **D**-unit is shown in red and the **A**-unit is shown in blue, CH…π interactions in **Hetero-4**, H atoms are shown in green, other hydrogen atoms and counter anions are omitted.

X-ray crystal data

Table S1. Crystal data and structure refinement for **Homo-1**.

Empirical formula	C93 H110 F12 N O28 Rh4 S8	
Formula weight	2627.96	
Temperature	173(2) K	
Wavelength	1.34138 Å	
Crystal system	Monoclinic	
Space group	C2/c	
Unit cell dimensions	a = 71.953(14) Å	α = 90°.
	b = 17.886(5) Å	β = 96.315(8)°.
	c = 37.342(8) Å	γ = 90°.
Volume	47767(19) $Å^3$	
Z	16	
Density (calculated)	1.462 Mg/m^3	
Absorption coefficient	4.328 mm^{-1}	
F(000)	21376	
Crystal size	0.390 x 0.080 x 0.040 mm^3	
Theta range for data collection	1.075 to 59.205°.	
Index ranges	-92<=h<=90, -21<=k<=22, -47<=l<=47	
Reflections collected	228175	
Independent reflections	51861 [R(int) = 0.0985]	
Completeness to theta = 53.594°	99.7 %	
Absorption correction	Semi-empirical from equivalents	
Max. and min. transmission	0.703 and 0.419	
Refinement method	Full-matrix least-squares on F^2	
Data / restraints / parameters	51861 / 222 / 2144	
Goodness-of-fit on F^2	1.061	
Final R indices [I>2sigma(I)]	R1 = 0.0854, wR2 = 0.2573	
R indices (all data)	R1 = 0.1527, wR2 = 0.3086	
Extinction coefficient	n/a	
Largest diff. peak and hole	1.438 and -1.432 $e.Å^{-3}$	

$R_1 = \Sigma||F0|-|Fc|| / \Sigma|F0|$ (based on reflections with $F_0^2 > 2\sigma F^2$). $wR_2 = [\Sigma[w(F_0^2-F_c^2)^2]/\Sigma[w(F_0)^2]]^{1/2}$; $w=1/[\sigma^2(F_0^2)+(0.095P)^2]$; $P = [\max(F_0^2,0)+2F_c^2]/3$(also with $F_0^2 > 2\sigma F^2$)

Table S2. Crystal data and structure refinement for **Homo-2**.

Empirical formula	C104.50 H125 F12 N13 O30.50 Rh4 S4	
Formula weight	2819.05	
Temperature	173(2) K	
Wavelength	1.34138 Å	
Crystal system	Triclinic	
Space group	P-1	
Unit cell dimensions	a = 17.0321(14) Å	α = 77.452(4)°.
	b = 18.8424(16) Å	β = 81.200(3)°.
	c = 39.863(3) Å	γ = 72.008(4)°.
Volume	11826.0(17) $Å^3$	
Z	4	
Density (calculated)	1.583 Mg/m^3	
Absorption coefficient	3.944 mm^{-1}	
F(000)	5756	
Crystal size	0.440 x 0.240 x 0.160 mm^3	
Theta range for data collection	2.689 to 55.000°.	
Index ranges	-20<=h<=20, -23<=k<=23, -48<=l<=48	
Reflections collected	135878	
Independent reflections	44422 [R(int) = 0.1185]	
Completeness to theta = 53.594°	98.5 %	
Absorption correction	Semi-empirical from equivalents	
Refinement method	Full-matrix least-squares on F^2	
Data / restraints / parameters	44422 / 357 / 2202	
Goodness-of-fit on F^2	1.151	
Final R indices [I>2sigma(I)]	R1 = 0.1512, wR2 = 0.3966	
R indices (all data)	R1 = 0.1977, wR2 = 0.4335	
Extinction coefficient	n/a	
Largest diff. peak and hole	3.565 and -2.382 $e.Å^{-3}$	

$R_1 = \Sigma||F0|-|Fc||$ (based on reflections with $F_0^2 > 2\sigma F^2$). $wR_2 = [\Sigma[w(F_0-F_c^2)^2]/\Sigma[w(F_0)^2]]^{1/2}$; $w=1/[\sigma^2(F_0^2)+(0.095P)^2]$; $P = [\max(F_0^2,0)+2F_c^2]/3$(also with $F_0^2 > 2\sigma F^2$)

Table S3. Crystal data and structure refinement for **Hetero-3**.

Empirical formula	C103 H107.50 F12 N12.50 O21.50 Rh4 S7	
Formula weight	2728.57	
Temperature	173(2) K	
Wavelength	1.34138 Å	
Crystal system	Monoclinic	
Space group	C2/c	
Unit cell dimensions	a = 67.429(5) Å	α = 90°.
	b = 23.8798(16) Å	β = 103.301(3)°.
	c = 29.2782(19) Å	γ = 90°.
Volume	45879(5) $Å^3$	
Z	16	
Density (calculated)	1.580 Mg/m^3	
Absorption coefficient	4.400 mm^{-1}	
F(000)	22160	
Crystal size	0.400 x 0.200 x 0.200 mm^3	
Theta range for data collection	3.141 to 54.995°.	
Index ranges	-82<=h<=82, -29<=k<=28, -35<=l<=35	
Reflections collected	200019	
Independent reflections	43546 [R(int) = 0.0540]	
Completeness to theta = 53.594°	99.9 %	
Absorption correction	Semi-empirical from equivalents	
Max. and min. transmission	0.657 and 0.367	
Refinement method	Full-matrix least-squares on F^2	
Data / restraints / parameters	43546 / 866 / 2419	
Goodness-of-fit on F^2	1.023	
Final R indices [I>2sigma(I)]	R1 = 0.0907, wR2 = 0.2814	
R indices (all data)	R1 = 0.1009, wR2 = 0.2944	
Extinction coefficient	n/a	
Largest diff. peak and hole	2.775 and -1.220 $e.Å^{-3}$	

$R_1 = \Sigma||F0|-|Fc|| / \Sigma|F0|$ (based on reflections with $F_0^2 > 2\sigma F^2$). $wR_2 = [\Sigma[w(F_0-F_c^2)^2]/\Sigma[w(F_0)^2]]^{1/2}$; $w=1/[\sigma^2(F_0^2)+(0.095P)^2]$; $P = [\max(F_0^2,0)+2F_c^2]/3$(also with $F_0^2>2\sigma F^2$)

Table S4. Crystal data and structure refinement for **Hetero-4**.

Empirical formula	C208 H264 F24 N26 O68 Rh8 S10	
Formula weight	5816.32	
Temperature	173(2) K	
Wavelength	1.34138 Å	
Crystal system	Triclinic	
Space group	P-1	
Unit cell dimensions	a = 22.383(4) Å	α = 92.104(7)°.
	b = 24.161(4) Å	β = 98.905(7)°.
	c = 24.592(4) Å	γ = 102.575(7)°.
Volume	12790(4) $Å^3$	
Z	2	
Density (calculated)	1.510 Mg/m^3	
Absorption coefficient	3.819 mm^{-1}	
F(000)	5948	
Crystal size	0.450 x 0.280 x 0.240 mm^3	
Theta range for data collection	2.760 to 56.000°.	
Index ranges	-27<=h<=27, -29<=k<=29, -30<=l<=30	
Reflections collected	232175	
Independent reflections	50484 [R(int) = 0.0784]	
Completeness to theta = 53.594°	99.8 %	
Absorption correction	Semi-empirical from equivalents	
Max. and min. transmission	0.579 and 0.348	
Refinement method	Full-matrix least-squares on F^2	
Data / restraints / parameters	50484 / 541 / 2687	
Goodness-of-fit on F^2	1.046	
Final R indices [I>2sigma(I)]	R1 = 0.1005, wR2 = 0.2969	
R indices (all data)	R1 = 0.1172, wR2 = 0.3201	
Extinction coefficient	0.00088(7)	
Largest diff. peak and hole	3.421 and -1.227 $e.Å^{-3}$	

$R_1 = \Sigma||F0|-|Fc|| / \Sigma|F0|$ (based on reflections with $F_0^2 > 2\sigma F^2$). $wR_2 = [\Sigma[w(F_0^2-F_c^2)^2]/\Sigma[w(F_0)^2]]^{1/2}$; $w=1/[\sigma^2(F_0^2)+(0.095P)^2]$; $P = [\max(F_0^2,0)+2F_c^2]/3$(also with $F_0^2 > 2\sigma F^2$)

References

[S1] Y. Lu, Y. J. Lin, Z. H. Li and G. X. Jin, *Chin. J. Chem.*, 2018, **36**, 106-111.

[S2] Y. Wang, W. G. Zhu, W. N. Du, X. F. Liu, X. T. Zhang, H. L. Dong and W. P. Hu, *Angew. Chem. Int. Edit.*, 2018, **57**, 3963-3967.

[S3] W. L. Shan, Y. J. Lin, F. E. Hahn and G. X. Jin, *Angew. Chem. Int. Ed.*, 2019, **58**, 5882-5886.